A variationally computed IR line list for the methyl radical CH$_3$

Ahmad Y. Adam,[†] Andrey Yachmenev,[‡] Sergei N. Yurchenko,[¶] and Per Jensen[*,†]

[†]*Fakultät für Mathematik und Naturwissenschaften, Physikalische und Theoretische Chemie, Bergische Universität Wuppertal, D–42097 Wuppertal, Germany*

[‡]*Center for Free-Electron Laser Science, Deutsches Elektronen-Synchrotron DESY, Notkestraße 85, D-22607 Hamburg, Germany, The Hamburg Center for Ultrafast Imaging, Universität Hamburg, Luruper Chaussee 149, D-22761 Hamburg, Germany*

[¶]*Department of Physics and Astronomy, University College London, Gower Street, London WC1E 6BT, United Kingdom*

E-mail: jensen@uni-wuppertal.de

Abstract

We present the first variational calculation of a ~~room~~ hot temperature *ab initio* line list for the CH$_3$ radical. It is based on a high level *ab initio* potential energy surface and dipole moment surface of CH$_3$ in the ground electronic state. The ro-vibrational energy levels and Einstein A coefficients were calculated using the general-molecule variational approach implemented in the computer program TROVE. Vibrational energies and vibrational intensities are found to be in very good agreement with the available experimental data. The line list comprises 9,127,123 ro-vibrational states ($J \leq 40$) and 2,058,655,166 transitions covering the wavenumber range up to 10000 cm^{-1} and should be suitable for temperatures up to $T = 1500$ K.

Introduction

The methyl radical is one of the most important free radicals and plays a central role in hydrocarbon combustion processes[?] in atmospheric chemistry,[?] in the chemistry of semiconductor production,[?] in the chemical vapor deposition of diamond,[?] and in many chemical processes of current industrial and environmental interest. It is also present in exo-planetary atmospheres,[?] in the atmospheres of Saturn[?] and Neptune,[?] and in the interstellar medium,[?] where it is thought to be one of the most abundant free radicals.[?] Because of its central role in this variety of situations, its structural and spectroscopic parameters have been the subject of numerous studies. A number of different spectroscopic techniques have been used to determine its absolute concentration in the gas phase, including UV/visible,[?] infrared,[?] and Raman spectroscopies.[? ? ? ? ? ? ?] In addition, CH_3 is an example of a molecule with large vibrational contribution to the hyperfine coupling constant, accounting for up to about 41% of the total value (see Ref. [?] and references therein).

Owing to the importance of CH_3 in various contexts, in particular in astrophysics and -chemistry, its concentrations or column densities in remote environments such as interstellar space, the terrestrial atmosphere, exo-planetary atmospheres, and the outer layers of cool stars are of interest and it is desirable to determine these by remote-sensing spectroscopic methods. A prerequisite for such determinations is the knowledge of the transition moments for the observed transitions, and these must often be obtained in theoretical calculations as done, for example, in the ExoMol project[? ?] by Yurchenko and co-workers.[? ? ? ? ? ? ? ? ? ? ? ?] This project aims at providing theoretically computed transition moments and simulated spectra for (small to medium-sized) general polyatomic molecules of astrophysical and/or -chemical interest.

At equilibrium, the three protons of electronic-ground-state $\tilde{X}\ ^2A_2''$ CH_3 form an equilateral triangle with the C nucleus at the centre-of-mass of the planar structure with $\boldsymbol{D}_{3h}$ point group symmetry (see Table A-10 of Ref. [?]). There is no permanent dipole moment, and so the pure rotational transitions are dipole forbidden and very weak. Also, the

planar ground-state equilibrium structure precludes most one-photon transitions to excited electronic states.[?] Owing to the extremely weak rotational spectrum, determinations of concentrations and column densities for CH_3 must be made with rovibrational transitions in the infrared region. The most suitable transitions are those in the intense ν_2 fundamental band at 606 cm^{-1} (where ν_2 is the out-of-plane bending mode). This band provides convenient transitions for concentration measurements and has been used extensively for this purpose.[?,?,?,?] As mentioned above, the corresponding transition moments must be known in order that concentrations can be determined, and the present work can be viewed as a first step towards providing extensive catalogues of theoretical transition moments for CH_3, so-called line lists, of use in astrophysical studies. In the present work we apply a high level *ab initio* potential energy surface, refined by means of experimental spectroscopic data, and *ab initio* dipole moment surfaces to compute, with the TROVE program,[?,?,?,?] sufficient energies and transition moments for generating a ~~room-temperature~~ hot ($T = 1500$ K) IR line list for CH_3.

Potential energy and dipole moment

Potential energy surface

The potential energy surface (PES) employed for the electronic ground state of CH_3 in the present work is based on the *ab initio* surface reported in Ref. [?], which we denote as PES-1. The PES-1 electronic energies were computed on a grid of 24 000 symmetry-unique molecular geometries employing the open-shell RCCSD(T)-F12b[?,?] level of theory (explicitly correlated F12 restricted coupled cluster included single and double excitations with a noniterative correction for triples) and the F12-optimized correlation consistent polarized valence basis set cc-pVQZ-F12.[?] In correlated calculations the carbon inner-shell electron pair was treated as frozen core. The analytical representation for the PES was obtained in a least-squares fitting procedure using the functional form from Lin *et al.*[?]:

$$V(\xi_1, \xi_2, \xi_3, \xi_{4a}, \xi_{4b}; \sin\bar\rho) \;=\; V_e + V_0(\sin\bar\rho) + \sum_j F_j(\sin\bar\rho)\,\xi_j$$
$$+ \sum_{j\leqslant k} F_{jk}(\sin\bar\rho)\,\xi_j\,\xi_k + \sum_{j\leqslant k\leqslant l} F_{jkl}(\sin\bar\rho)\,\xi_j\,\xi_k\,\xi_l$$
$$+ \sum_{j\leqslant k\leqslant l\leqslant m} F_{jklm}(\sin\bar\rho)\,\xi_j\,\xi_k\,\xi_l\,\xi_m + \ldots\,; \tag{1}$$

this function is expressed in terms of the stretching variables

$$\xi_k = 1 - \exp\left[-a(r_k - r_e)\right], \quad k = 1, 2, 3, \tag{2}$$

where r_k is the instantaneous value of the distance between the C nucleus and the proton H_k labeled $k = 1$, 2, or 3; r_e is the common equilibrium value of the three r_k bond lengths, and a is a Morse parameter. Furthermore, the symmetrized bending variables (ξ_{4a}, ξ_{4b}) are defined as

$$(\xi_{4a}, \xi_{4b}) = \left(\frac{1}{\sqrt{6}}[2\,\alpha_1 - \alpha_2 - \alpha_3], \frac{1}{\sqrt{2}}[\alpha_2 - \alpha_3]\right) \tag{3}$$

with α_i as the bond angle $\angle(H_jXH_k)$ where (i, j, k) is a permutation of the numbers (1,2,3). Finally, the variable

$$\sin\bar\rho = \frac{2}{\sqrt{3}}\,\sin[(\alpha_1 + \alpha_2 + \alpha_3)/6] \tag{4}$$

describes the out-of-plane bending. At the planar equilibrium configuration, we have $\alpha_1 + \alpha_2 + \alpha_3 = 360°$ and so $\sin\bar\rho = \sin\bar\rho_e = 1$. The functions $V_0(\sin\bar\rho)$ and $F_{jk\ldots}(\sin\bar\rho)$ in Eq. (1) are defined as

$$V_0(\sin\bar\rho) \;=\; \sum_{s=1}^{4} f_0^{(s)}\,(1 - \sin\bar\rho)^s, \tag{5}$$

$$F_{jk\ldots}(\sin\bar\rho) \;=\; \sum_{s=0}^{N} f_{jk\ldots}^{(s)}\,(1 - \sin\bar\rho)^s, \tag{6}$$

4

67 where the quantities $f_0^{(s)}$ and $f_{jk...}^{(s)}$ in Eqs. (5) and (6) are expansion coefficients. The opti-

68 mized values of the parameters a, r_e, $f_0^{(s)}$, and $f_{jk...}^{(s)}$ are given in the supplementary material

69 to Ref. **?** together with Fortran 90 routine for calculating PES values.

70   The analytical form of PES-1**?** is given in terms of the *ab initio* cc-pVQZ-F12 values of

71 the equilibrium structural parameters, $r_\mathrm{e} = 1.0774$ Å and $\alpha_\mathrm{e} = 120.0°$,**?** for the electronic

72 ground state of CH_3. In the present work, we optimized the values r_e and α_e in a least-squares

73 fitting to experimentally derived to rotational energy spacings within the vibrational states

74 of CH_3. The fitting produced the values of $r_\mathrm{e} = 1.0763$ Å and $\alpha_\mathrm{e} = 120.0$. We adopt

75 these optimized values of the equilibrium structural parameters. All results presented in the

76 remainder of the present work are based on the analytical potential energy function called

77 PES-2, obtained from PES-1**?** by replacing the *ab initio* cc-pVQZ-F12 values of r_e and α_e

78 by the adjusted values given here. The remaining PES-2 parameter values are identical to

79 those of PES-1 and can be obtained from the supplementary material to Ref. **?** .

80 # Dipole moment surface

81 The dipole moment surface (DMS) for the electronic ground state of CH_3 was computed

82 using the MOLPRO**?** program package. Frozen-core calculations were carried out for $19\,361$

83 symmetry-unique geometries ($15\,600$ below $30\,000$ cm^{-1}) using the spin-restricted open-shell

84 coupled cluster theory RCCSD(T)**?** and the augmented correlation consistent valence ba-

85 sis set aug-cc-pVTZ,**? ?** employing the two-point stencil central finite differences with the

86 electric field strength of 0.002 a.u.

    We employ the so-called symmetrized molecular-bond (SMB) representation**?** [which is

an extension of the molecular-bond (MB) representation**?**] to formulate analytical functions

describing the molecular dipole moment components. The SMB representation makes use

of the projections $\bar{\boldsymbol{\mu}} \cdot \mathbf{e}_k$ of the dipole moment on the molecular bonds, where $\mathbf{e}_k$ is the unit

vector along the C–H$_k$ bond,

$$\mathbf{e}_k = \frac{\mathbf{r}_k - \mathbf{r}_4}{|\mathbf{r}_k - \mathbf{r}_4|} \tag{7}$$

87 with $\mathbf{r}_k$, $k = 1, 2, 3$, as the position vector of proton k and $\mathbf{r}_4$ as the position vector of the

88 C nucleus.

89 We form symmetry-adapted linear combinations of the MB projections $\bar{\boldsymbol{\mu}} \cdot \mathbf{e}_j$:

$$\bar{\mu}_{A_2''}^{\mathrm{SMB}} = (\bar{\boldsymbol{\mu}} \cdot \mathbf{e}_{\mathrm{N}}) \tag{8}$$

$$\bar{\mu}_{E_a'}^{\mathrm{SMB}} = \frac{1}{\sqrt{6}} \left[2 (\bar{\boldsymbol{\mu}} \cdot \mathbf{e}_1) - (\bar{\boldsymbol{\mu}} \cdot \mathbf{e}_2) - (\bar{\boldsymbol{\mu}} \cdot \mathbf{e}_3) \right] \tag{9}$$

$$\bar{\mu}_{E_b'}^{\mathrm{SMB}} = \frac{1}{\sqrt{2}} \left[(\bar{\boldsymbol{\mu}} \cdot \mathbf{e}_2) - (\bar{\boldsymbol{\mu}} \cdot \mathbf{e}_3) \right], \tag{10}$$

where, in addition to the vectors $\mathbf{e}_k$, we have introduced $\mathbf{e}_{\mathrm{N}} = \mathbf{q}_{\mathrm{N}}/|\mathbf{q}_{\mathrm{N}}|$ with $\mathbf{q}_{\mathrm{N}}$ as the 'trisector'

$$\mathbf{q}_{\mathrm{N}} = (\mathbf{e}_1 \times \mathbf{e}_2) + (\mathbf{e}_2 \times \mathbf{e}_3) + (\mathbf{e}_3 \times \mathbf{e}_1). \tag{11}$$

90 The subscripts $\Gamma = A_2''$, E_a', and E_b' of the quantities $\bar{\mu}_{\Gamma}^{\mathrm{SMB}}$ in Eqs. (8)–(10) refer to the

91 irreducible representations (Table A-10 of Ref. **?**) of the CH_3 molecular symmetry group

92 $\boldsymbol{D}_{3\mathrm{h}}(\mathrm{M})$; the electronically averaged dipole moment $\bar{\boldsymbol{\mu}}$ generates the representation $A_2'' \oplus$

93 E'. The quantity $\bar{\mu}_{A_2''}^{\mathrm{SMB}}$ is antisymmetric under the inversion operation[?] E^* and vanishes

94 at planarity, so that $\bar{\boldsymbol{\mu}}$ has only two non-vanishing, linearly independent components at

95 planarity. These two components vanish at planar configurations with $\boldsymbol{D}_{3\mathrm{h}}$ point group

96 symmetry.

The three components of the SMB dipole moment in Eqs. (8)–(10) are represented by 4th order polynomial expansions

$$\begin{aligned} \bar{\mu}_{\Gamma}^{\mathrm{SMB}}(\chi_1, \chi_2, \chi_3, \chi_{4a}, \chi_{4b}; \rho) = {} & \mu_0^{\Gamma}(\sin \bar{\rho}) + \sum_i \mu_i^{\Gamma}(\sin \bar{\rho})\chi_i + \sum_{i \leq j} \mu_{ij}^{\Gamma}(\sin \bar{\rho})\chi_i \chi_j \\ & + \sum_{i \leq j \leq k} \mu_{ijk}^{\Gamma}(\sin \bar{\rho})\chi_i \chi_j \chi_k + \sum_{i \leq j \leq k \leq l} \mu_{ijkl}^{\Gamma}(\sin \bar{\rho})\chi_i \chi_j \chi_k \chi_l, \end{aligned} \tag{12}$$

in terms of the variables

$$\chi_k = \Delta r_k (1 - \exp(-\Delta r_k))^2, \quad (k = 1, 2, 3) \tag{13}$$

with $\Delta r_k = r_k - r_e$ and

$$(\chi_4, \chi_5) = (\xi_{4a}, \xi_{4b}) \tag{14}$$

where (ξ_{4a}, ξ_{4b}) are defined in Eq. (3). The expansion coefficients $\mu_{ij\ldots}^{\Gamma}(\sin\bar{\rho})$ are defined as

$$\mu_{ij\ldots}^{\Gamma}(\sin\bar{\rho}) = \sum_{s=0}^{N} \mu_{ij\ldots}^{\Gamma(s)}(1 - \sin\bar{\rho})^s, \tag{15}$$

where $\sin\bar{\rho}$ is given by Eq. (4) and the maximal order of the polynomial is $N = 8$. For more details the reader is referred to Ref. ? . The final fit of the $15\,600$ geometries required a total number of 218 parameters (131 for $\bar{\mu}_{A_2''}^{\mathrm{SMB}}$ and 87 for $\bar{\mu}_{E_a'}^{\mathrm{SMB}}$ and $\bar{\mu}_{E_b'}^{\mathrm{SMB}}$) and reproduced the *ab initio* data with a root-mean-square (RMS) differences of 0.003 D, 0.001 D and 0.004 D for the x, y and z components respectively and energies up to $30\,000$ cm^{-1}, see 1. A series of fittings to the x, y and z *ab initio* dipole-moment components have been carried out, including in the data set for each fitting the *ab initio* points with electronic energy (relative to the potential energy minimum) $V \leqslant E$, and increasing E. 1 shows the RMS deviation for each dipole-moment component as a function of E. The DMS expansion parameter set and the Fortran 90 functions are included in the supplementary material.

Intensity simulations with TROVE

General expressions

The 'readiness' of the molecule to make an absorption or emission transition from an initial ro-vibrational state i to a final ro-vibrational state f is expressed by the line strength[?][?][?] $S(f \leftarrow i)$, a quantity with units of [dipole moment]^2 (typically Debye^2). For $S(f \leftarrow i) = 0$, the transition does not take place and need not be considered. As discussed in Ref. ? transitions with $S(f \leftarrow i) \neq 0$ are said to satisfy selection rules which we can derive from symmetry considerations before we do quantitative, numerical calculations of $S(f \leftarrow i)$. Thus, these calculations need only be done for transitions satisfying the selection rules, and

Figure 1: Root-mean-square (RMS) errors of the fittings to the *ab initio* dipole moment values. The results of a series of fittings are shown. In each fitting, the data set includes the *ab initio* points with electronic energy (relative to the potential energy minimum) $V \leqslant E$ (see text).
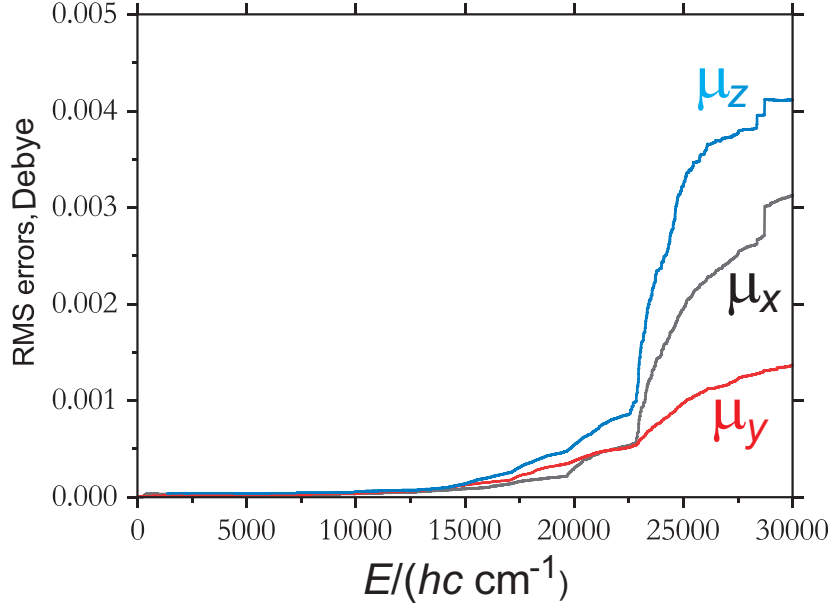
after obtaining values of $S(f \leftarrow i)$ for these transitions, we can compute the corresponding Einstein coefficients and absorption intensities.

The initial(final) state $i(f)$ has the rotation-vibration wavefunction $|\Phi_{\mathrm{rv}}^{(i)}\rangle(|\Phi_{\mathrm{rv}}^{(f)}\rangle)$. The line strength[?][?][?] $S(f \leftarrow i)$ of the ro-vibrational transition $f \leftarrow i$ is

$$S(f \leftarrow i) = g_{\mathrm{ns}} \sum_{M_f, M_i} \sum_{A=X,Y,Z} \left| \left\langle \Phi_{\mathrm{rv}}^{(f)} \left| \bar{\mu}_A \right| \Phi_{\mathrm{rv}}^{(i)} \right\rangle \right|^2, \tag{16}$$

where g_{ns} is the nuclear spin statistical weight factor[?] and $\bar{\mu}_A$ is the electronically averaged component of the molecular dipole moment along the space-fixed axis[?] $A = X$, Y, or Z. The quantum numbers M_i and M_f are the projections of the total angular momentum $\hat{\mathbf{J}}$ on the Z axis for the initial and final states, respectively.

8

Assuming that the molecules considered are in thermal equilibrium at the absolute temperature T, the intensity of a spectral line is determined as

$$I(f \leftarrow i) = \frac{8\pi^3 N_A \tilde{\nu}_{if}}{(4\pi\epsilon_0)3hc} \frac{\mathrm{e}^{-E_i/kT}}{Q} \left[1 - \exp(-hc\tilde{\nu}_{if}/kT)\right] S(f \leftarrow i). \qquad (17)$$

Here $\tilde{\nu}$ is the absorption wavenumber, and Eq. (17) refers to the transition from the state i with energy E_i to the state f with energy E_f, where $hc\tilde{\nu}_{if} = E_f - E_i$. Q is the partition function defined as $Q = \sum_j g_j \exp(-E_j/kT)$, where g_j is the total degeneracy of the state with energy E_j and the sum runs over all energy levels of the molecule, and other symbols have their usual meanings. The total degeneracy g_j is given by $(2J + 1)$ times the spin degeneracy $(M = 2)$ and times the nuclear spin degeneracy which is 4, 0, 2, 4, 0, 2 for A_1', A_2', E', A_1'', A_2'', and E'' symmetries respectively. The ground electronic state of CH_3 is a doublet $(\tilde{X}\ ^2A_2'')$ with a small splitting[?][?] in the rovibrational energy levels due to spin-rotation interactions, around 0.01 cm^{-1}, which we therefore chose to ignore for this work, byt however scaling the line intensities by the spin-multiplicity factor of 2.

A detailed expression for the line strength of an individual ro-vibrational transition within an isolated electronic state of an XY$_3$ pyramidal molecule is given in Eq. (21) of Yurchenko *et al.*[?] Provided that the population of the lower (initial) state is defined by the Boltzmann distribution, ~~it is sufficient to~~ we consider only transitions starting from the levels below $E_i^{\max}/hc = \cancel{39\,200}000$ cm^{-1}, which corresponds to Boltzmann factors of ~~$\exp(-E_i/kT) > 2 \times 10^{-7}$~~ $\exp(-E_i/kT) > 2 \times 10^{-4}$ entering into Eq. (17) for ~~$T = 300$~~ $T = 1500$ K. It is common to use the partition function for estimating the completeness of the line list for a given temperature[?]. By considering the ratio $Q_{9000\,\mathrm{cm}^{-1}}/Q_{\mathrm{total}}$, where Q_{total} is the converged partition function value calculated by explicitly summing over all energy levels and $Q_{9000\,\mathrm{cm}^{-1}}$ is the partition function calculated using only those levels with energies up to the threshold of 9000 cm^{-1}. This ratio gives 95 % completeness at temperatures below 1500 K, which we estimate as the maximal temperature for our line list. For similar reasons, the

¹⁴⁴ range of the rotational excitations can be safely limited at ~~$J = 26$~~ $J = 40$. The wavenumber

¹⁴⁵ range selected is 0 to ~~8~~10 000 cm^{-1}; the upper energy limit (i.e., the maximal energy for the

¹⁴⁶ final state) corresponds to a term value of $E^{\mathrm{max}}/hc = $ ~~12~~19,000 cm^{-1}.

Computational details

¹⁴⁸ We use a symmetry-adapted basis set in the variational nuclear motion calculations. The

¹⁴⁹ Hamiltonian matrix is factorized into size-independent blocks according to the irreducible

¹⁵⁰ representations of the $\boldsymbol{D}_{3\mathrm{h}}(\mathrm{M})$ molecular symmetry group:[?] A_1', A_2', A_1'', A_2'', E', and E''.

¹⁵¹ The A_2' and A_2'' matrices are of no interest for CH$_3$ as the corresponding states have zero

¹⁵² nuclear spin statistical weights and do not exist in Nature.[?] The E' and E'' matrices each

¹⁵³ split into two sub-blocks, of which only one must be diagonalized.[?]

The calculation of the matrix elements $\langle \Phi_{\mathrm{rv}}^{(f)} | \bar{\mu}_A | \Phi_{\mathrm{rv}}^{(i)} \rangle$ in Eq. (16) is the bottle-neck in

the spectrum simulations. Here, the wavefunctions $\Phi_{\mathrm{rv}}^{(w)}$ are expressed as symmetry-adapted

linear combinations of basis functions (see Eq. (65) of Yurchenko *et al.*[?]):

$$|\Phi_{\mathrm{rv}}^{(w)}\rangle = \sum_{VK\tau_{\mathrm{rot}}} C_{VK\tau_{\mathrm{rot}}}^{(w)} |J_w\, K\, m_w\, \tau_{\mathrm{rot}}\rangle\, |V\rangle, \quad w = i \ \text{ or } \ f, \tag{18}$$

¹⁵⁴ where the $C_{VK\tau_{\mathrm{rot}}}^{(w)}$ are expansion coefficients, $|J_w\, K\, m_w\, \tau_{\mathrm{rot}}\rangle$ is a symmetrized rotational basis

¹⁵⁵ function, τ_{rot} (= 0 or 1) is associated with the rotational parity, and $|V\rangle$ is a vibrational

¹⁵⁶ basis function. In order to speed up this part of the calculations, we applied a pre-screening

¹⁵⁷ procedure to the expansion coefficients $C_{VK\tau_{\mathrm{rot}}}^{(f)}$. All terms with coefficients less than the

¹⁵⁸ threshold value of ~~10^{-22}~~ 10^{-13} were excluded from the integration.

A speedup in the evaluation of the dipole moment matrix elements $\langle \Phi_{\mathrm{rv}}^{(f)} | \bar{\mu}_A | \Phi_{\mathrm{rv}}^{(i)} \rangle$ can

be done in two steps. First, for a given lower state i the following effective line strength is

evaluated:

$$S_{i,VK}^{A} = \langle \Phi_{\mathrm{rv}}^{(i)} | \bar{\mu}_A | \phi_{VK} \rangle, \tag{19}$$

where we introduced a short-hand notation ϕ_{VK} for the primitive basis function $|J_w K\, m_w\, \tau_{\mathrm{rot}}\rangle$

$\times|V\rangle$. Once all $S_{i,VK}$ are computed, in the second step the line strength $S(f \leftarrow i)$ is evaluated as

$$S(f \leftarrow i) = g_{\text{ns}} \sum_{m_i,m_f} \sum_{A=X,Y,Z} \left| \sum_{V,K} C^{(f)}_{VK\tau_{\text{rot}}} S^A_{i,VK} \right|^2 . \tag{20}$$

We had to compute a very large number of transitions satisfying the selection rule $|J_f - J_i|$ $\leqslant 1$, where J_i and J_f are the values of the angular momentum quantum number J for the initial and final state, respectively. Consequently, we saved memory by organizing the calculation of the ro-vibrational eigenstates and the $S(f \leftarrow i)$-values such that at a given time, only eigenvectors for states with two consecutive J-values, J and $J+1$, are available for the computation of $S(f \leftarrow i)$-values. This algorithm is implemented in the GPU GAIN-MPI program [?].

The vibrational basis set $|V\rangle$ is obtained in TROVE using a multi-step contraction and symmetrization procedure, starting from local primitive basis set functions, each depending on one variable only (see Refs. [?] [?] [?] and references therein). Thus, a compact representation of the vibrational basis set is obtained in a form optimized for the molecule of interest. The final vibrational basis set is represented by the eigenfunctions of the purely vibrational part of the Hamiltonian; we call these eigenfunctions the '$J = 0$ basis'.

Results

Basis set convergence and empirical adjustment of the vibrational band centers

The dimensions of the Hamiltonian matrix blocks to be diagonalized are important in determining the accuracy with which highly excited ro-vibrational energies and wavefunctions can be computed, and consequently it is important to derive by empirical methods the smallest basis set that is consistent with the required eigenvalue accuracy (that is to say, the optimum size for 'convergence').

TROVE employs polyad number truncation[?][?][?] to control the size of the vibrational basis set, with the polyad number P given by:

$$P = 2(n_1 + n_2 + n_3) + n_4 + n_5 + n_6, \tag{21}$$

where n_i are the quantum numbers connected with the primitive functions $\phi_{n_i}(\xi_i)$. That is, we include in the primitive basis set only those functions $\phi_{n_i}(\xi_i)$ for which $P \leq P_{\max}$.

The vibrational term values could be converged even more tightly by extrapolating the energies calculated with different-size basis sets $P_{\max}$ to the complete vibrational basis set limit.[?] However, this is not considered necessary for the purpose of generating a line list since the corrections from such an extrapolation will be small compared with the inherent errors in the term values that are caused by the imperfection of the underlying potential energy surface. Instead, if we aim for higher accuracy in a pragmatic manner, we can resort to a more empirical approach where the theoretical vibrational term values are replaced by accurate experimental vibrational band centres, whenever these are available in the literature. In this case, we adjust the vibrational band centers 'by hand', and by doing so, we shift the rotational energy structure towards better agreement with experiment. This procedure can be regarded as an empirical basis set correction scheme and will be denoted as EBSC scheme.

We adopt the EBSC scheme for the vibrational bands $2\nu_2$, ν_1, ν_4^1, and ν_3^1, for which accurate experimental data is available, in combination with PES-2, where we have adjusted the equilibrium structure of the molecule to fit the experimentally derived pure rotational term values. The vibrational basis set was truncated at the polyad number $P_{\max} = 32$. The incorporation of experimental information in the EBSC scheme is obviously a departure from a purely *ab initio* approach which is considered to be justified by the gain in accuracy that can be achieved when computing an extensive ro-vibrational line list.

To achieve higher accuracy for the vibrational band centers, another more thorough refinement of our PES would be needed. However, considering a severe lack of the accurate

experimental data on the vibrationally excited states of CH_3, we decided for a pragmatic, alternative procedure based on the EBSC substitution scheme in conjunction with the r_e-refinement. Even though we cannot avoid imperfections for all bands which where not EBSC-corrected, a more accurate rotational structure should be useful for assignments of future experimental works on CH_3.

1 lists the vibrational band centers of methyl radical up to $5000~\mathrm{cm}^{-1}$, as derived from experimental data and from variational calculations of the present work computed using PES ~~2 in conjunction~~ 2. These experimental band centers were used to replace the theoretical values $P_{\max} = 32$ values in all $J > 0$ TROVE calculations according with the EBSC substitution. This table also shows the effect of the polyad-number on the vibrational energy.

2 shows a comparison of the pure rotational energies ($J \leq 5$) of CH_3 before and after refinement of r_e illustrating the importance of this step.

The vibrational transition moments are defined as

$$\mu_{V'V} = \sqrt{\sum_{\alpha=x,y,z} |\langle V' \mid \bar{\mu}_\alpha \mid V \rangle|^2} \tag{22}$$

where $|V'\rangle$ and $|V\rangle$ denote $J = 0$ vibrational wavefunctions and $\bar{\mu}_\alpha$ is the electronically-averaged dipole moment in the molecular frame (see the section entitled 'Dipole moment surface' above). For calculation of vibrational transition moments we used our *ab initio* PES-1 and truncated the vibrational basis set at polyad number $P_{\max} = 32$. A number of computed transition moments for the strongest lower lying bands are listed in Table 3 where they are compared with the available experimental data The complete list of theoretical transition moments is given as Supporting Information and can be also found at `www.exomol.com`.

_____

13

Table 1: Vibrational band centers (cm^{-1}) of $^{12}\text{CH}_3$ from variational calculations.

Γ	State	Ref.	Obs.[a]	$P_{\max} = 24$[b]	$P_{\max} = 32$[c]
A_1'	$2\nu_2$	?	1288.1	1279.77	1281.24
	$2\nu_4$			2737.63	2739.64
	$4\nu_2$			2773.65	2776.86
	ν_1	?	3004.42	3002.71	3002.76
	$3\nu_4^3$			4118.59	4120.58
	$\nu_1 + 2\nu_2$			4258.97	4260.53
	$6\nu_2$			4391.99	4397.00
	$\nu_3^1 + \nu_4^1$			4537.94	4538.93
	$4\nu_4$			5371.39	5364.56
	$2\nu_2 + 3\nu_4^3$			5475.84	5480.07
	$4\nu_2 + 2\nu_4$			5601.91	5607.20
E'	ν_4^1	?	1397.0	1385.99	1387.26
	$2\nu_2 + \nu_4^1$			2688.80	2691.61
	$2\nu_4^2$			2759.77	2762.05
	ν_3^1	?	3160.8	3158.88	3158.83
	$3\nu_4^1$			4074.69	4075.46
	$2\nu_2 + 2\nu_4^2$			4087.92	4091.72
A_2''	ν_2	?	606.453	602.43	602.43
	$3\nu_2$			2010.09	2010.09
	$\nu_2 + 2\nu_4^0$			3372.27	3371.59
	$5\nu_2$			3569.96	3569.95
	$\nu_1 + \nu_2$			3596.35	3596.30
	$3\nu_4^3$			4768.70	4767.06
	$\nu_2 + 2\nu_4^0$			4823.32	4822.79
	$\nu_1 + 3\nu_2$			4981.58	4981.52
E''	$\nu_2 + \nu_4^1$			2000.24	2002.22
	$\nu_2 + 2\nu_4^2$			3388.24	3391.11
	$3\nu_2 + \nu_4^1$			3426.45	3430.06
	$\nu_2 + \nu_3^1$			3736.40	3736.97
	$\nu_2 + 3\nu_4^1$			4726.62	4728.62
	$3\nu_2 + 2\nu_4^2$			4835.22	4839.85
	$\nu_1 + \nu_2 + \nu_4^1$			4980.92	4983.16

[a] Experimental values of band centers used to replace the theoretical values $P_{\max} = 32$, see text.
[b] Computed using the $P_{\max} = 24$ basis set in conjunction with PES-2.[?]
[c] Computed using the $P_{\max} = 32$ basis set in conjunction with PES-2.[?]

Table 2: Theoretical rotational term values ($N \leq 5$, in cm^{-1}) of CH$_3$, computed with TROVE using different equilibrium structure parameters.

States			Term values		
N	K	τ_{rot}	Obs.	Obs.-Calc.^{a}	Obs.-Calc.^{b}
1	1	0	14.3189	0.032377	0.004027
2	0	1	57.4396	0.112005	-0.002023
2	2	0	38.1186	0.092340	0.017004
2	1	0	52.6112	0.106875	0.002511
3	3	0	71.3965	0.179934	0.038989
3	2	0	95.5353	0.203902	0.014649
3	1	0	110.0032	0.219365	0.001200
4	0	0	191.2473	0.375024	-0.004034
4	4	0	114.1491	0.295456	0.070301
4	2	0	172.0038	0.353500	0.012772
4	3	0	147.9203	0.327970	0.035289

^{a} Calculated using $r_{\mathrm{e}} = 1.07736927$ Å and $\alpha_{\mathrm{e}} = 120.0°$ (PES-1, see text).
^{b} Calculated using $r_{\mathrm{e}} = 1.0762977119$ Å and $\alpha_{\mathrm{e}} = 120.0°$ (PES-2, see text).

Intensity simulations

In order to simulate absorption spectra at a given temperature T and within a particular wavenumber range, the upper and lower energies and the Einstein coefficients $A(f \leftarrow i)$ [or the line strengths $S(f \leftarrow i)$; the relationship between $A(f \leftarrow i)$ and $S(f \leftarrow i)$ is described in Ref. **?**] of all transitions in this range must be known; in practice, only the transitions above a certain minimum intensity are included. The simplest way to present the spectral data is a 'stick' diagram where the height gives the integrated absorption coefficient from Eq. (17). In this section we report such simulations for the CH$_3$ absorption bands covering the frequency range 600–1200 cm^{-1} for the out-of-plane bending mode ν_2. The line strengths in Eq. (17) are computed from Eq. (16) with the spin statistical weights g_{ns} from Ref. **?** . The simulations are carried out using PES-2 and the computed DMS described above. We used a partition-function value of $Q = $ ~~724.6306~~732.734, obtained at 300 K by summing over all variational term values $(J \leq 40)$ below 36871.73 cm^{-1}. With the limits defined above, we computed ~~22 805 378 transitions .~~ 2,058,655,166 transitions using the GPU GAIN-MPI

Table 3: Band Centers ν_{fi} and Vibrational Transition Moments μ_{fi} for CH_3.[a]

States		$\nu_{fi}/\mathrm{cm}^{-1}$	Calc. μ_{fi}/D	Obs. μ_{fi}/D	Ref.
f	i				
$2\nu_2$	ν_2	678.81	0.25684	0.31(6)	[?]
ν_2	0	602.43	0.20403	0.215(25)	[? ? ?]
ν_3^1	0	3158.83	0.03999	0.03(27)	[? ?]
ν_4^1	0	1387.26	0.02931		
$2\nu_3 + \nu_4$	0	4529.74	0.02049		
$\nu_1 + \nu_4^1$	0	4383.56	0.00866		
$2\nu_2 + \nu_3^1$	0	4396.18	0.00486		
$2\nu_3^2$	0	6294.76	0.00462		
$\nu_1 + \nu_3^1$	0	6076.68	0.00321		
$2\nu_4^2$	0	2762.05	0.00313		
$\nu_3^1 + 2\nu_4$	0	5864.94	0.00242		
$3\nu_4^1$	0	4075.46	0.00186		
$2\nu_2 + \nu_3^1 + \nu_4^1$	0	5789.16	0.00130		
$4\nu_2$	0	5856.39	0.00116		

[a] The transitions originate in the vibrational ground state ($i = 0$) with the exception of the hot band $2\nu_2 \leftarrow \nu_2$.

237 program.[?]

238   2 gives an overview (log-scale) of the absorption spectrum of CH_3 at ~~T = 300 K~~ different

239 temperatures produced using the line list (log-scale) by means of the ExoCross program.[?]

240 3 shows four regions with the strongest, dipole-allowed bands ν_2, ν_4, ν_3 and $\nu_3 + \nu_4$.

Figure 2: An overview of the absorption spectrum (cross sections) of CH_3 at ~~T = 300~~ different temperatures $T = 300, 500, 1000$ and 1500 K generated using our line list and the Gaussian line profile with the full-width-at-half-maximum of ~~2~~1 cm^{-1}.
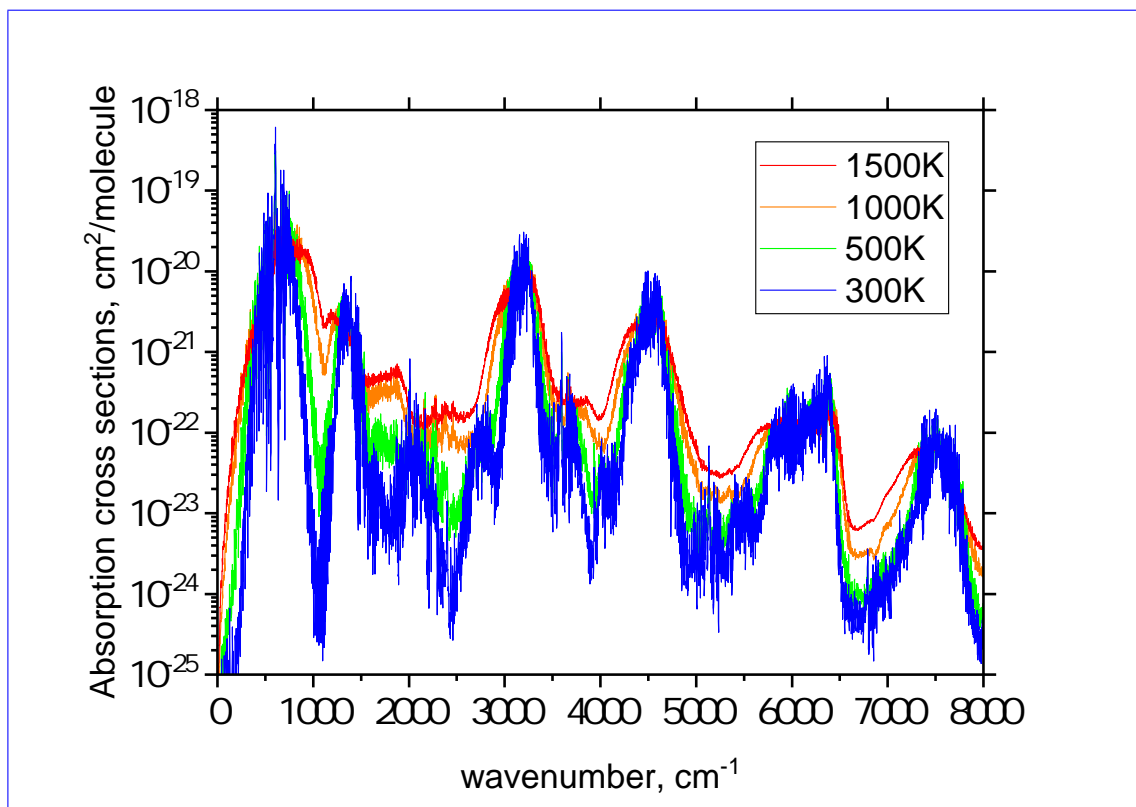
241   4 shows the emission spectrum of CH_3 in the wavenumber interval 600-1200 cm^{-1}, sim-

242 ulated with TROVE at two different levels of theory, rovibrational and purely vibrational.

243 The simulated spectra are compared to an experimental spectrum recorded by Hermann and

244 Leone[? ?] (see Fig. 4 of Ref. [?]).

245   4(a) shows a simulation of the CH_3 emission spectrum, computed with TROVE at a tem-

246 perature of $T = 300$ K, taking into account all vibrational transitions in the 600-1200 cm^{-1}

247 interval that are calculated with the $P_{\max} = 32$ basis set. The simulation involves the con-

Figure 3: A selection of the strongest absorption bands of CH_3 at $T = 296$ K generated using the line list. A Gaussian line profile with the half-width-half-maximum of 0.08 cm^{-1} was used in production of the cross sections shown.
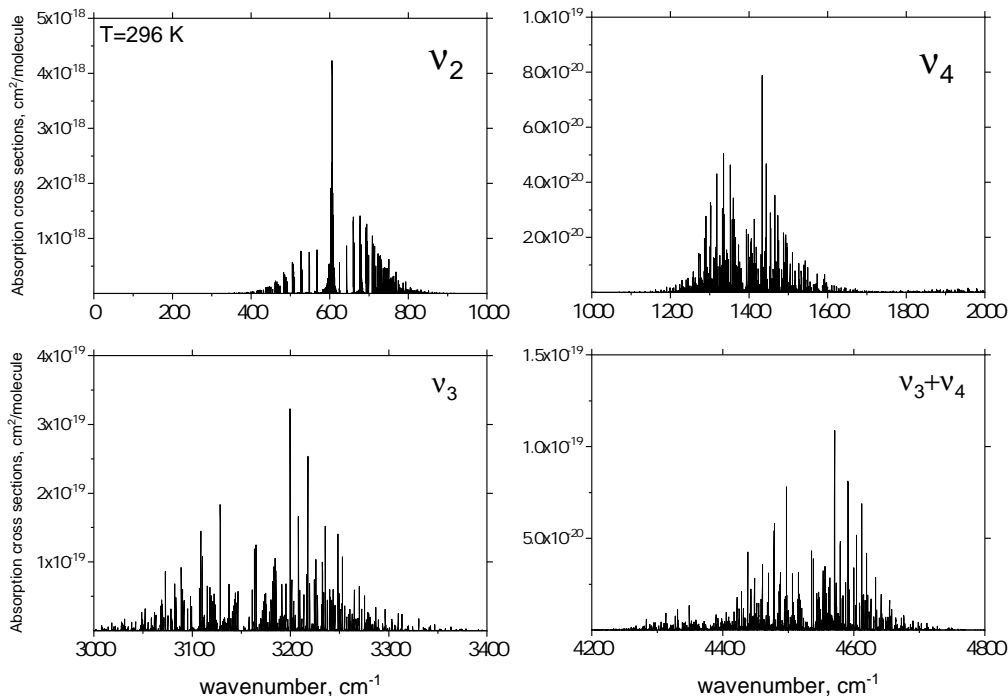
volution of the calculated intensities with a Gaussian line shape function with a full width at half maximum (FWHM) of 17 cm^{-1}.

The simulation is compared with the experimental spectrum obtained by Hermann and Leone,[?][?] shown in 4(b).* In the experiment, the CH_3 radicals were produced the in a photo-fragmentation process of methyl iodide CH_3I. Hermann and Leone[?][?] suggested that after the breaking of the C–I bond, the CH_3 radicals are predominantly produced in excited states of the out-of-plane bending mode ν_2. The CH_3 fragment of a dissociated CH_3I molecule will typically have a pyramidal structure close to that of the methyl group in CH_3I. For a CH_3 radical, however, which is planar at equilibrium, such structures are associated with high excitations of the ν_2 vibrational mode. Excitations with $v_2 \leqslant 10$ have been observed in the

---

*Reproduced from Hermann, H. W.; Leone, S. R. The Journal of Chemical Physics 1982, 76, 4759–4765, with the permission of AIP Publishing.

[258] emission experiment of Refs. ? ? .

[259-264] ~~The low-temperature line list generated for CH_3 in the present work does not cover an energy interval large enough to allow an accurate simulation of~~ In order to simulate vibrationally very hot transitions (hotter than 1500 K) corresponding to the experimental spectrum of Refs. ? which involves out-of-plane bending states $v_2\,\nu_2$ with $v_2 \leqslant$ ~~10. We have circumvented this problem by carrying out simulations of the experimental spectrum~~ 10, we have carried out simulations employing a so-called one-band model (with the one band being the ν_2 fundamental band here). In the one-band model, we use the ν_2-band data from the 'parent', 300 K ro-vibrational line list also for the hot bands accompanying the ν_2 band. The procedure employed is detailed in Ref. ? and we outline it briefly here: We initially produce the 300 K, ν_2-band cross sections by means of the ExoCross program? and convolve them with a Gaussian profile of FWHM = 17 cm^{-1} between 0 and 1200 cm^{-1}, generating 1201 data points. Then the wavenumbers of the computed cross sections are shifted by -606.4531 cm^{-1}, positioning the band center at zero, and the cross sections are normalized. A local version of ExoCross now obtains, from the vibrational transition moments computed with TROVE, the vibrational band intensities for the hot bands $(v_2 + 1)\,\nu_2 \leftarrow v_2\,\nu_2$, $v_2 \leqslant$ 9. Finally, the simulated spectrum is generated by placing, for each hot band, the ν_2-band profile at the band center ν_{fi} of the hot band in question, scaled by its vibrational band intensity. Such simulations have been carried out for temperatures T of 1000, 2000, and 3000 K, respectively, and the results are shown in 4(c), where they can be compared to the experimental results[?,?] in 4(b).

[279] 4(c) shows that the 'standard' $T = 300$ K rovibrational simulation of the CH_3 emission spectrum [4(a)] has little resemblance to the experimental spectrum from Ref. ? [4(b)]. Obviously in the experiment, the CH_3 molecules populate states of much higher energies than those accessed in thermal equilibrium at $T = 300$ K. However, among the 'vibrational simulations' in 4(c), the curve obtained for $T = 2000$ K has a very substantial similarity to the experimental curve. This confirms the suggestion by Hermann and Leone[?,?] that dis-

sociation of CH_3I produces CH_3 radicals in highly excited states of the out-of-plane bending mode ν_2. The successful simulation of the emission spectrum of Refs. **?** **?** lends credibility to the *ab initio* DMS of the present work; the intensities based on this DMS are in very good qualitative agreement with experiment.

Our complete ~~$T = 300$~~ $T = 1500$ K CH_3 line list is ~~given as Supporting Information~~ accessed via the repository `www.zenodo.org`, see Ref. **?** . It details the transition energies, line strengths, ~~and~~ Einstein coefficients $A(f \leftarrow i)$ ~~, together with the absorption intensities estimated for $T = 300$~~ and the temperature dependent partition function $Q(T)$. The line list should be applicable for the temperatures below 1500 K. However, the simulated spectra will become increasingly inaccurate with increasing temperature. The line list is given using the ExoMol format **?** which can be used together with the ExoCross program **?** to generate spectra of CH_3.

Conclusion

We have presented calculated spectra for the methyl radical covering a large part of the infrared region. Detailed comparisons with observed room-temperature spectra show excellent agreement for the position and intensity of the transitions.

Our ultimate aim is the construction of a CH_3 line list capable of reproducing and predicting observed spectra at temperatures much higher than 300 K. This will facilitate detections of the methyl radical in space. The work presented here represents the first step towards this goal, which involves the generation, refinement, and validation of the required potential energy and dipole moment surfaces, as well as establishing the level of accuracy that can be achieved in the variational nuclear-motion calculations with our computational resources. In this initial phase, we have produced an methyl radical line list consisting of ~~22.8 million transitions between 3,671,465~~ 2 billion transitions between 9,127,123 energy levels for ro-vibrational states up to $J_{\max} = $ ~~25~~ 40 and energies up to ~~20~~ 19 000 cm^{-1}. ~~Even though this~~

310 ~~list is less complete and less accurate than ultimately desired, it can be used to produce~~

311 ~~simulated CH₃ spectra that agree well with observation at room temperature.~~

Figure 4: Emission spectra of CH_3. (a) Rovibrational simulation assuming the CH_3 radicals to be in thermal equilibrium at $T = 300$ K. (b) CH_3 (ν_2) out-of-plane bending mode emission spectrum (dots) obtained[?] after dissociation of $CH_3I \rightarrow CH_3(\nu_2) + I^*$. The continuous curve is the best fit[?] involving the hot bands $(v_2 + 1)\,\nu_2 \leftarrow v_2\,\nu_2$ with $v_2 \leqslant 9$. The spectrum is convolved with a spectrometer slit function with a FWHM of 33 cm^{-1} and a 19 cm^{-1} bandwidth ascribed to the breadth of the $\Delta K = 0$ manifold of transitions with varying J values. Reproduced from Ref. [?] with the permission of AIP Publishing. (c) Vibrational simulations at temperatures $T = 1000$, 2000, and 3000 K, respectively, taking into account the vibrational transitions $(v_2 + 1)\,\nu_2 \leftarrow v_2\,\nu_2$ with $v_2 \leqslant 9$ (see text).

Supporting Information Available

The Supporting Information for this work includes: (i) dipole moment parameters $\mu_{k,l,m,\ldots}^{(\Gamma)}$, (ii) potential energy parameters $f_{jk\ldots}^{(s)}$; (iii) Fortran routines for calculating the dipole moment and potential energy values for a given geometry. Our complete $T = 1500\mathrm{K}$ CH$_3$ line list together with the partition function can be accessed via the Zenodo repository, www.zenodo.org [?] as well as at www.exomol.com.

FIGURE CAPTIONS

1. Root-mean-square (RMS) errors of the fittings to the *ab initio* dipole moment values. The results of a series of fittings are shown. In each fitting, the data set includes the *ab initio* points with electronic energy (relative to the potential energy minimum) $V \leqslant E$ (see text).

2. An overview of the absorption spectrum (cross sections) of CH_3 at ~~$T = 300$~~ different temperatures $T = 300, 500, 1000$ and 1500 K generated using our line list and the Gaussian line profile with the full-width-at-half-maximum of ~~2 cm^{-1}~~ 1 cm^{-1}.

3. A selection of the strongest absorption bands of CH_3 at $T = 296$ K generated using the line list. A Gaussian line profile with the half-width-half-maximum of 0.08 cm^{-1} was used in production of the cross sections shown.

4. Emission spectra of CH_3. (a) Rovibrational simulation assuming the CH_3 radicals to be in thermal equilibrium at $T = 300$ K. (b) CH_3 (ν_2) out-of-plane bending mode emission spectrum (dots) obtained[?] after dissociation of $CH_3I \rightarrow CH_3(\nu_2)$ + I*. The continuous curve is the best fit[?] involving the hot bands $(v_2 + 1)\nu_2 \leftarrow v_2\nu_2$ with $v_2 \leqslant 9$. The spectrum is convolved with a spectrometer slit function with a FWHM of 33 cm^{-1} and a 19 cm^{-1} bandwidth ascribed to the breadth of the $\Delta K = 0$ manifold of transitions with varying J values. Reproduced from Fig. 4 of Ref. [?] with the permission of AIP Publishing. (c) Vibrational simulations at temperatures $T = 1000, 2000$, and 3000 K, respectively, taking into account the vibrational transitions $(v_2 + 1)\nu_2 \leftarrow v_2\nu_2$ with $v_2 \leqslant 9$ (see text).